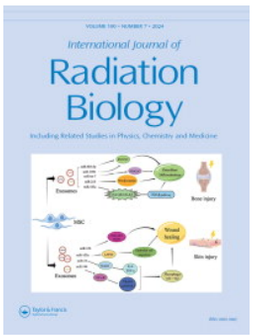

International Journal of Radiation Biology

ISSN: (Print) (Online) Journal homepage: www.tandfonline.com/journals/irab20

Comparative analysis of the yields of dicentrics and chromosomal translocations

Dorota Młynarczyk, Pedro Puig, Joan F. Barquinero, Carmen Armero & Virgilio Gómez-Rubio

To cite this article: Dorota Młynarczyk, Pedro Puig, Joan F. Barquinero, Carmen Armero & Virgilio Gómez-Rubio (02 Jul 2024): Comparative analysis of the yields of dicentrics and chromosomal translocations, International Journal of Radiation Biology, DOI: 10.1080/09553002.2024.2369077

To link to this article: https://doi.org/10.1080/09553002.2024.2369077

INTERNATIONAL JOURNAL OF RADIATION BIOLOGY
https://doi.org/10.1080/09553002.2024.2369077

Taylor & Francis
Taylor & Francis Group

ORIGINAL ARTICLE

OPEN ACCESS Check for updates

Comparative analysis of the yields of dicentrics and chromosomal translocations

Dorota Młynarczyk[a], Pedro Puig[a,b], Joan F. Barquinero[c], Carmen Armero[d] and Virgilio Gómez-Rubio[e]

[a]Departament de Matemàtiques, Universitat Autònoma de Barcelona, Bellaterra, Spain; [b]Centre de Recerca Matemàtica, Bellaterra, Spain; [c]Departament de Biologia Animal, Biologia Vegetal i Ecologia, Universitat Autònoma de Barcelona, Bellaterra, Spain; [d]Departament d'Estadística i Investigació Operativa, Universitat de València, València, Spain; [e]Department of Mathematics, School of Industrial Engineering, Universidad de Castilla-La Mancha, Albacete, Spain

ABSTRACT

Purpose: Chromosomal dicentrics and translocations are commonly employed as biomarkers to estimate radiation doses. The main goal of this article is to perform a comparative analysis of yields of both types of aberrations. The objective is to determine if there are relevant distinctions between both yields, allowing for a comprehensive assessment of their respective suitability and accuracy in the estimation of radiation doses.

Materials and methods: The analysis involved data from a partial-radiation simulation study with the calibration data obtained through two scoring methods: conventional and PAINT modified. Subsequently, a Bayesian bivariate zero-inflated Poisson model was employed to compare the posterior marginal density of the mean of dicentrics and translocations and assess the differences between them.

Results: When employing the conventional method of scoring, the findings indicate that there is no notable disparity between the yield of observed translocations and dicentrics. However, when utilizing the PAINT modified method, a notable discrepancy is observed for higher doses, indicating a relevant difference in the mean number of the two types of aberrations.

Conclusions: The choice of scoring method significantly influences the analysis of radiation-induced aberrations, especially when distinguishing between complex and simple chromosomal formations. Further research and analysis are necessary to gain a deeper understanding of the factors and mechanisms impacting the formation of dicentrics and translocations.

ARTICLE HISTORY
Received 15 November 2023
Revised 9 April 2024
Accepted 29 May 2024

KEYWORDS
Bivariate zero-inflated Poisson model; FISH-painting; PAINT and conventional nomenclatures; radiation-induced chromosome aberrations

1. Introduction

The quantitative assessment of dicentrics and translocations, two well-studied chromosomal aberrations induced by exposure to ionizing radiation, plays a pivotal role in radiation biology. Sometimes, it is assumed that yields for these two types of aberrations are very similar, but concerns may arise regarding their potential inequality, highlighting the complex mechanisms that influence these chromosomal changes in response to varying radiation doses. The current radiation biodosimetry manual (IAEA 2011) recommends that each laboratory should develop its own fitting dose–response curves for translocations, but, in practice, in situations where a laboratory lacks a specific translocations curve, it is occasionally acceptable to use the calibration curve for dicentrics (Moquet et al. 2000; Edwards et al. 2005). Furthermore, the analysis of aberrations may also be influenced by the detection technique employed and the terminology used to characterize these alterations (Knehr et al. 1998, 1999). Thus, the objective of this article is to compare yields for dicentrics and translocations obtained using different scoring systems, with the aim of evaluating the technique's influence on the disparities between these yields. While some authors have previously tackled this issue (Lindholm et al. 1998; Barquinero et al. 1999), our current article emphasizes a new mathematical approach.

Radiation-induced chromosome exchange aberrations produced in lymphocytes in G0 (quiescent) stage have been classified as symmetrical or asymmetrical (i.e. reciprocal translocations or dicentrics) (Savage and Papworth 1982). For biological dosimetry purposes and in solid stained metaphases, symmetrical exchanges are difficult to detect, unless the resulting chromosomes are markedly different from the normal karyotype. For this reason, initially biological dosimetry was based on the detection of dicentrics or dicentrics plus rings (IAEA 2001). From the visualization of a solid stained dicentric plus its corresponding acentric fragment, it was logical to infer that this exchange resulted to the

CONTACT Dorota Młynarczyk dorotaanna.mlynarczyk@uab.cat Departament de Matemàtiques, Universitat Autònoma de Barcelona, Bellaterra, Spain.
Supplemental data for this article can be accessed online at https://doi.org/10.1080/09553002.2024.2369077.

interaction of two broken chromosomes, and by association the same for symmetric exchanges like translocations. The introduction of fluorescence in situ hybridization (FISH) techniques to detect whole chromosomes (chromosome-painting) allowed an easy detection of translocations (Lucas et al. 1992). However, with the same technique, it was evident that radiation-induced chromosome exchanges could be formed by the interaction of more than two breaks (Cremer et al. 1990; Schmid et al. 1992) and exchanges were classified between simple and complex. The former involves two breaks and the latter involving three or more breaks in two or more chromosomes (Savage and Simpson 1994).

The first calibration curves produced by chromosome-painting used the terms translocation and dicentric similarly to that was done when analyzing solid stained metaphases (Lucas et al. 1992; Bauchinger et al. 1993; Fernández et al. 1995), i.e. distinguishing aberrations: translocation (*t*), dicentric (*dic*), ring (*r*), insertion (*ins*), and additional acentric (*ace*) fragment (ISCN 1985). This system, hereafter referred to as the conventional system, may also identify complete or incomplete dicentrics and translocations, along with centric or acentric rings. However, the presence of complex exchanges mainly at higher doses led the development of specific nomenclatures to describe the radiation-induced exchanges. Initially, two highly different nomenclatures were proposed: the nomenclature with the acronym PAINT (from Protocol for Aberration Identification and Nomenclature Terminology; Tucker et al. 1995) was purely descriptive of each abnormal piece present in the metaphase, without cross-reference to other aberrant pieces in the same metaphase; and the CAB terminology (from Chromosomes-Arms-Breaks; Cornforth 2001) or the so-called S&S system (Savage and Simpson 1994) that proposed a code with numerals and letters that refer to the number of abnormal pieces observed and how common the exchange was expected to be. Understanding complex aberrations is greatly aided by the CAB terminology, which focused on the mechanical aspects of exchange formation. However, in daily practice, the use of the CAB vocabulary was not easy to handle, and currently the most widely used method to score the chromosome exchanges using FISH is to describe each abnormal metaphase as a unit using the PAINT nomenclature in a slightly modified way that allows to infer the mechanistic aspects of exchange formation and allows classifying between simple and complex aberrations (Knehr et al. 1998). Specifically, within the PAINT modified system, terms like 'apparently simple dicentric/translocation' (ASD/AST) are employed to describe aberrations involving bicolored chromosomes with single-color junctions each (Tucker et al. 1995), which may be the result of complex, undetected aberrations.

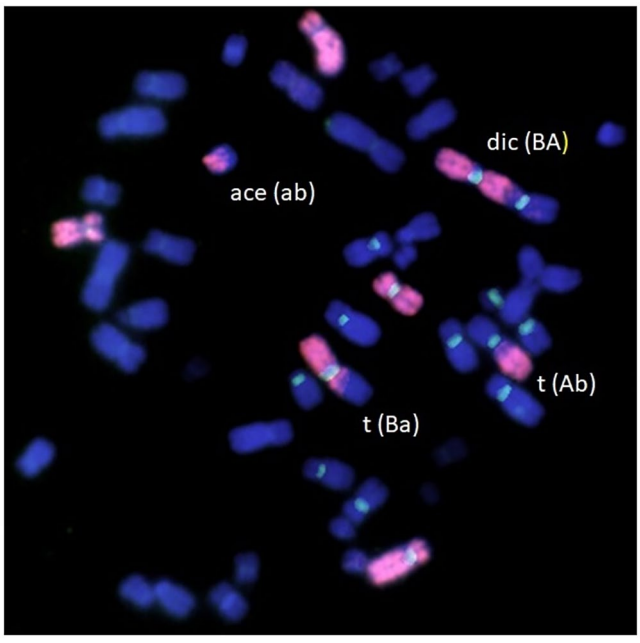

Figure 1. An example of a metaphase illustrating FISH-based chromosome 'painting'. In red painted chromosomes #1, #4, and #11, in blue counterstained chromosomes.

Despite the existence of these nomenclatures, some biological dosimetry laboratories still rely on conventional terminology to describe chromosomal alterations. To illustrate the problem, let us consider an example from Figure 1. The metaphase contains four aberrant pieces with painted material involved. The metaphase would be scored as: *dic*(BA), *t*(Ba), *ace*(ab), and *t*(Ab). These aberrations could be scored by combining aberrations that imply the minimum number of breaks, i.e. *dic*(BA) with *ace*(ab), which is an ASD or a dicentric, and *t*(Ba) with *t*(Ab), which is an AST or a translocation. However, one could also combine *dic*(BA) with *t*(Ab), resulting in a complex aberration (neither ASD nor AST), and it will be counted as one dicentric plus one translocation in the conventional nomenclature. Similarly, combining *t*(Ba) with *ace*(ab) results in a complex aberration, which will be counted as a translocation. Therefore, the question is how different scoring systems (conventional vs. PAINT modified) influence the analysis of yields of aberrations, and whether these can lead to misleading interpretations of the results. These misinterpretations could have a strong impact in past or chronic dose–assessments by biological dosimetry using FISH techniques. This issue has been highlighted in interlaboratory comparisons (Lee et al. 2021; Barquinero et al. 2023).

2. Materials and methods

For the purpose of this research, we decided to utilize the data obtained from the study conducted by Duran et al. (2002). The study involved a blood sample taken from a healthy 32-year-old male that were exposed to X-rays at radiation doses of 2, 3, 4, and 5 Gy within a laboratory environment. Subsequent to the exposure, the samples underwent the FISH protocol with chromosomes 1, 4, and 11 being painted. The scoring of chromosomal aberrations was carried out using both the conventional and PAINT modified methods. This implies that we have counts of dicentrics and translocations via the conventional scoring approach, as well as counts of ASD and AST using the PAINT modified approach for each cell, what enables a comparison between the results obtained from both methods.

Duran et al. (2002) studied specifically partial body radiation exposures. This type of exposure occurs when only a specific region or part of the body is subjected to radiation, such as during targeted radiation therapy or accidental exposure to a localized radiation source. To replicate this situation experimentally, blood irradiated at 2, 3, 4 and 5 Gy was mixed with non-irradiated blood in proportions of: 0.875, 0.75, 0.5, 0.25, and 0.125. Furthermore, the analysis also considered the impact of total irradiation by including samples with a proportion of 1 (without the addition of non-irradiated blood to the samples). To obtain chromosome spreads, blood was cultured during 48 h, and colcemid was added 2 h before harvesting. To detect chromosome exchanges Cy-3 labeled probes for chromosomes 1, 4 and 11 and a FITC-labeled pancentromeric probe were used to distinguish between chromosome exchanges carrying one centromere (i.e. translocations) or chromosome exchanges involving two or more centromeres (i.e. dicentrics) (more details of the experiment can be found in Duran et al. 2002). Subsequently, these mixed samples were carefully scored using both considered terminologies.

Table 1 displays the mean number of aberrations for each dose and dilution p (proportion of irradiated cells), utilizing both the conventional and PAINT mod. nomenclature. In total, 20,332 cells were scored, with the lowest count of 3,733 at a dose of 5 Gy and of 1,302 for proportion p = 1. This table highlights relevant differences between the two scoring systems under consideration as evident in the variations in the mean numbers of dicentrics/ASD and translocations/AST. The raw data can be found in the supplementary material of this article.

From a statistical standpoint, the bivariate Poisson model seems to be a suitable choice when working with both dicentrics and translocations, as it allows for joint analysis and inference about the underlying processes. This model assumes that both count variables are generated by two different Poisson processes, with a specific correlation term between them. Moreover, the bivariate Poisson model can be extended to cover scenarios with partial body exposures. The experimental design, which combines irradiated and non-irradiated samples, results in a significant number of zero counts in the observed data, which can be effectively handled by a bivariate zero-inflated Poisson model. While bivariate Poisson models have been widely employed for analyzing sports and healthcare data (Karlis and Ntzoufras 2003), their application in the field of biodosimetry has been largely unexplored. Furthermore, the bivariate approach utilized in this study for analyzing dicentrics and translocations can also be applied to analyze dicentrics and rings or dicentrics and foci. However, it would be more difficult in the case of foci due to their significant dependence on the amount of time that has passed following irradiation (Młynarczyk et al. 2022).

To begin the probabilistic formulation of the sampling model, let us clarify that we are defining a single model for both scoring techniques. Therefore, in this section, we will simply refer to aberrations as dicentrics and translocations, without mentioning ASD or AST. Assume that N cells were examined. We denote the number of dicentrics X_j and of translocations Y_j found in cell j, $j=1,\ldots,N$. Then, it is assumed that X_j and Y_j jointly follow a conditional zero-inflated bivariate Poisson distribution, with probability function:

$$f_{ZIBP}(x_j,y_j\mid\omega,\lambda_{1j},\lambda_{2j},\lambda_{3j}) = \begin{cases} \omega f_{BP}(x_j,y_j\mid\lambda_{1j},\lambda_{2j},\lambda_{3j}) & (x_j,y_j)\neq(0,0) \\ (1-\omega)+\omega f_{BP}(x_j,y_j\mid\lambda_{1j},\lambda_{2j},\lambda_{3j}) & (x_j,y_j)=(0,0) \end{cases} \quad (1)$$

where $(1-\omega)$ is the proportion of structural zeros (proportion of not-irradiated cells), and $f_{BP}(x_j,y_j\mid\lambda_{1j},\lambda_{2j},\lambda_{3j})$ is the conditional probability function of the bivariate Poisson distribution given by

$$f_{BP}(x_j,y_j\mid\lambda_{1j},\lambda_{2j},\lambda_{3j}) = \exp(-(\lambda_{1j}+\lambda_{2j}+\lambda_{3j})) \times\frac{\lambda_{1j}^{x_j}}{x_j!}\frac{\lambda_{2j}^{y_j}}{y_j!}\sum_{k=0}^{\min(x_j,y_j)}\binom{x_j}{k}\binom{y_j}{k}k!\left(\frac{\lambda_{3j}}{\lambda_{1j}\lambda_{2j}}\right)^k.$$

The effect on the irradiated cells is determined by the parameters λ_{1j},λ_2, and λ_{3j} in our model. In more detail, $\lambda_{1j}+\lambda_{3j}$ represents the marginal mean of the number of dicentrics, $\lambda_{2j}+\lambda_{3j}$ the marginal mean of translocations, and λ_{3j} the covariance term between the number of dicentrics and translocations (all them for the irradiated cells). These parameters, all them greater than zero, can be modeled as functions of the radiation dose using a regression approach.

Table 1. Mean number of aberrations for each dose and dilution p, utilizing both the conventional and PAINT mod. scoring systems.

	Dose (Gy)	2	2	2	2	2	2	3	3	3	3	3	3
	Proportion of irradiated cells p	1	0.875	0.75	0.50	0.25	0.125	1	0.875	0.75	0.50	0.25	0.125
	Number of cells	525	974	1551	1322	1516	1322	394	509	824	1009	1070	1096
Conventional	Mean dicentrics	0.12	0.07	0.06	0.04	0.02	0.01	0.21	0.22	0.10	0.08	0.03	0.02
	Mean translocations	0.11	0.08	0.06	0.05	0.02	0.01	0.27	0.21	0.10	0.10	0.03	0.04
PAINT mod.	Mean ASD	0.10	0.07	0.06	0.04	0.02	0.01	0.16	0.21	0.10	0.07	0.03	0.02
	Mean AST	0.08	0.07	0.05	0.04	0.02	0.01	0.20	0.17	0.08	0.07	0.02	0.03
	Dose (Gy)	4	4	4	4	4	4	5	5	5	5	5	5
	Proportion of irradiated cells p	1	0.875	0.75	0.50	0.25	0.125	1	0.875	0.75	0.50	0.25	0.125
	Number of cells	250	463	504	775	1035	1040	133	374	553	523	890	1260
Conventional	Mean dicentrics	0.48	0.23	0.16	0.10	0.04	0.02	0.47	0.35	0.20	0.11	0.06	0.02
	Mean translocations	0.50	0.20	0.19	0.12	0.04	0.02	0.59	0.30	0.18	0.13	0.06	0.02
PAINT mod.	Mean ASD	0.38	0.20	0.14	0.08	0.04	0.01	0.33	0.27	0.18	0.08	0.05	0.02
	Mean AST	0.33	0.16	0.14	0.08	0.03	0.02	0.42	0.20	0.13	0.09	0.04	0.01

The mean number of aberrations is frequently estimated in biodosimetric research using a linear or quadratic function of dose; we chose to concentrate on the quadratic model because the linear model is also included in it. We specify them as,

$$\begin{array}{cc} \text{dicentrics} & \lambda_{1j} = \beta_{11} + \beta_{12}\cdot d_j + \beta_{13}\cdot d_j^2, \\ \text{translocations} & \lambda_{2j} = \beta_{21} + \beta_{22}\cdot d_j + \beta_{23}\cdot d_j^2, \\ \text{covariance} & \lambda_{3j} = \beta_{31}, \end{array} \tag{2}$$

where d_j denotes the radiation dose received by jth cell, and $\beta_{\cdot\cdot}$ denotes the corresponding regression coefficients. The expected number of dicentrics, including irradiated and not-irradiated cells, is $\mu_{1j} = E(X_j \mid \beta_{11},\beta_{12},\beta_{13}) = \omega(\lambda_{1j} + \lambda_{3j})$. Similarly for translocations $\mu_{2j} = E(Y_j \mid \beta_{21},\beta_{22},\beta_{23}) = \omega(\lambda_{2j} + \lambda_{3j})$.

It has been studied that some cells exposed to radiation fail to survive until the metaphase stage of the cell cycle, when dicentrics and translocations are analyzed (Hall and Giaccia 2006). As a result, the actual proportion of irradiated cells present in the sample at the time of the analysis is lower than the initially assumed proportion. This discrepancy between both proportions poses a challenge in accurately assessing the radiation-induced chromosomal aberrations. Therefore, it is essential to account for this limitation, so researchers employ a statistical correction to estimate the true proportion of irradiated cells (Pujol et al. 2016). The survival rate, the proportion of the irradiated cells which survive until the metaphase, is described as a decreasing exponential function of the dose:

$$s(d) = \exp(-\gamma d),$$

where γ is the so-called survival index, $\gamma \in [0,1]$. Therefore, the actual proportion ω of scored cells irradiated at dose d is given by (see Supplementary Material for details)

$$\omega(d,p) = \frac{1}{1+\exp(\gamma d)(1-p)/p}, \tag{3}$$

where p is the initial proportion of the irradiated cells. Note that in the given experiment d and p are known, but the survival index γ needs to be estimated.

Let us denote by $\mathbf{x} = (x_1,\ldots,x_N)$ the counts of dicentrics in cells $1,\ldots,N$, and respectively the counts of translocations by $\mathbf{y} = (y_1,\ldots,y_N)$. The vector $\boldsymbol{d} = (d_1,\ldots,d_N)$ stands for the radiation doses to which each cell was exposed and $\boldsymbol{p} = (p_1,\ldots,p_N)$ is the vector of initial proportion of irradiated cells in the sample from which the observation comes. Thus, the likelihood of the model is given by

$$\begin{aligned} L(\mathbf{x},\mathbf{y},\boldsymbol{d},\boldsymbol{p} \mid \boldsymbol{\beta},\gamma) = \prod_{j=1}^{N} \Bigg(& 1_{(0,0)}(x_j,y_j)\left(1 - \frac{1}{1+\exp(\gamma d_j)(1-p_j)/p_j}\right) \\ & + \frac{1}{1+\exp(\gamma d_j)(1-p_j)/p_j} \exp(-(\lambda_{1j}+\lambda_{2_j}+\lambda_{3j}))\frac{\lambda_{1j}^{x_j}}{x_j!}\frac{\lambda_{2j}^{y_j}}{y_j!} \\ & \times \sum_{k=0}^{\min(x_j,y_j)} \binom{x_j}{k}\binom{y_j}{k} k! \left(\frac{\lambda_{3j}}{\lambda_{1j}\lambda_{2j}}\right)^k \Bigg), \end{aligned}$$

where λ_{ij} is defined in Equation (2), and $1_{(0,0)}(x_j,y_j)$ is an indicator function that is 1 when $x_j = y_j = 0$ and 0 otherwise. Within the Bayesian framework, the main interest is in computing the posterior distribution $\pi(\boldsymbol{\beta},\gamma \mid \mathbf{x},\mathbf{y},\boldsymbol{d},\boldsymbol{p})$ of the parameters of the model, i.e. the regression coefficients $\boldsymbol{\beta} = (\beta_{11},\ldots,\beta_{31})$ and the survival index γ, through the Bayes' theorem:

$$\pi(\boldsymbol{\beta},\gamma \mid \mathbf{x},\mathbf{y},\boldsymbol{d},\boldsymbol{p}) \propto L(\mathbf{x},\mathbf{y},\boldsymbol{d},\boldsymbol{p} \mid \boldsymbol{\beta},\gamma)\pi(\boldsymbol{\beta},\gamma),$$

where $\pi(\boldsymbol{\beta},\gamma)$ is the prior distribution for $(\boldsymbol{\beta},\gamma)$. We assume prior independence between $\boldsymbol{\beta}$ and γ, so $\pi(\boldsymbol{\beta},\gamma) = \pi(\boldsymbol{\beta})\pi(\gamma)$. Given the fact that λ_{1j} and λ_{2j} should be non-negative, the prior distribution $\pi(\boldsymbol{\beta})$ was chosen to be a non-informative uniform distribution on the interval (0, 10). The prior distribution for γ was chosen to be a uniform distribution on the interval [0,1] because, according to the definition, the survival index belongs to the interval [0,1]. Approximated samples from the posterior distribution $\pi(\boldsymbol{\beta},\gamma \mid \mathbf{x},\mathbf{y},\boldsymbol{d},\boldsymbol{p})$ were generated using Markov chain Monte Carlo methods. The JAGS software (Plummer 2003), in particular, was utilized with specific configurations, including the use of two chains, conducting 25,000 simulations, burn-in of 1000 iterations, and thinning every 25 iterations (the program itself is available in the Supplementary Material).

Note that λ_{1j} and λ_{2j} depend on the dose received by the cell j and are determined by Equation (2). By fixing the dose and utilizing samples from the posterior distribution, it becomes straightforward to derive the posterior distribution for the expected number of aberrations. From this point onward, we will focus only on the irradiated cells (with the actual proportion $\omega(d,p) = 1$), since we regard this as the most interesting case. For a fixed dose d, we can omit the subindex j in Equation (2), and denote the mean number of dicentrics of the irradiated cells for dose d as μ_{1d} and of translocations as μ_{2d}. Our main goal is to discuss whether these mean values differ from each other. To do so, we can consider the posterior distribution of the difference between means $\pi(\mu_{1d} - \mu_{2d} \mid \mathbf{x},\mathbf{y},\boldsymbol{d},\boldsymbol{p})$. It can be easily approximated through simulation, enabling the calculation of the posterior mean of the difference, credible intervals, and conducting graphical analysis by plotting posterior densities for each dose. We will report highest density intervals (HDIs), which are credible intervals designed to have a higher probability density for all values inside the interval compared to those outside (Kruschke 2014).

We can additionally compare the models by assessing the probability that the mean number of dicentrics of the irradiated cells, μ_{1d}, is lower than the mean number of translocations, μ_{2d}, separately calculated for each dose d. Let us define this as hypothesis $H_1 : \mu_{1d} - \mu_{2d} < 0$. Conversely, the alternative scenario will be denoted as H_2, with $H_2 : \mu_{1d} - \mu_{2d} \geq 0$. Evaluating the ratio between the posterior probability of H_1 and that of H_2, i.e.

$$\frac{\pi(\mu_{1d} - \mu_{2d} < 0 \mid \mathbf{x},\mathbf{y},\boldsymbol{d},\boldsymbol{p})}{\pi(\mu_{1d} - \mu_{2d} \geq 0 \mid \mathbf{x},\mathbf{y},\boldsymbol{d},\boldsymbol{p})} \tag{4}$$

may assist us in determining which situation is more likely. Given our prior assumption that both hypotheses are equally probable a priori, i.e. $P(H_1) = P(H_2) = 0.5$, this resulting odds can be interpreted as the Bayes factor (Kass and Raftery 1995) (details can be found in Supplementary Material). According to the Jeffreys scale (Jeffreys 1961), a Bayes factor close to 1 suggests only 'bare mention' evidence of a difference between μ_{1d} and μ_{2d}. A number greater than 3 but less than 10 is considered 'substantial' evidence. Results between 10 and 30 indicate 'strong' evidence, and between 30 and 100 are categorized as 'very strong.' A Bayes factor exceeding 100 is considered 'decisive.'

3. Results

Our objective is to examine the feasibility of employing the same calibration curve for both dicentrics and translocations, which entails comparing the parameters μ_{1d} and μ_{2d} defined in Section 2. Figure 2 depicts the posterior distribution of the means of the number of dicentrics μ_{1d} and translocations μ_{1d} for conventional scoring method and for ASD and AST for PAINT modified technique, across different doses. Notably, this information reveals that the posterior mean values of dicentrics and translocations are relatively similar when using conventional nomenclature. The density of dicentrics of the irradiated cells is skewed to the left for each dose compared to translocations. Conversely, in the case of the PAINT modified scoring, the posterior distribution for AST is shifted toward the left. This difference becomes more pronounced as the dose increases, indicating a relevant difference between them, as can also be noticed looking at Figure 3. This figure represents the posterior density of the difference between estimated means of dicentrics and translocations (or ASD and AST), $\pi(\mu_{1d} - \mu_{2d} \mid \mathbf{x}, \mathbf{y}, \boldsymbol{d}, \boldsymbol{p})$ for the irradiated cells at each dose and for both scoring techniques. Posterior mean and 95% HDI intervals of the differences for each case can be found in Table 2. All of these findings indicate that there are some distinctions in the means, especially in the case of a dose of 4 Gy for the PAINT mod. method. Nevertheless, it's important to mention that more noticeable differences can be detected at higher doses.

The results presented in Table 3 showcase the posterior odds, defined previously (Equation (4)), as the ratio of probabilities between instances where μ_{1d} is lower than μ_{2d} and vice versa. However, for a more robust interpretation of the

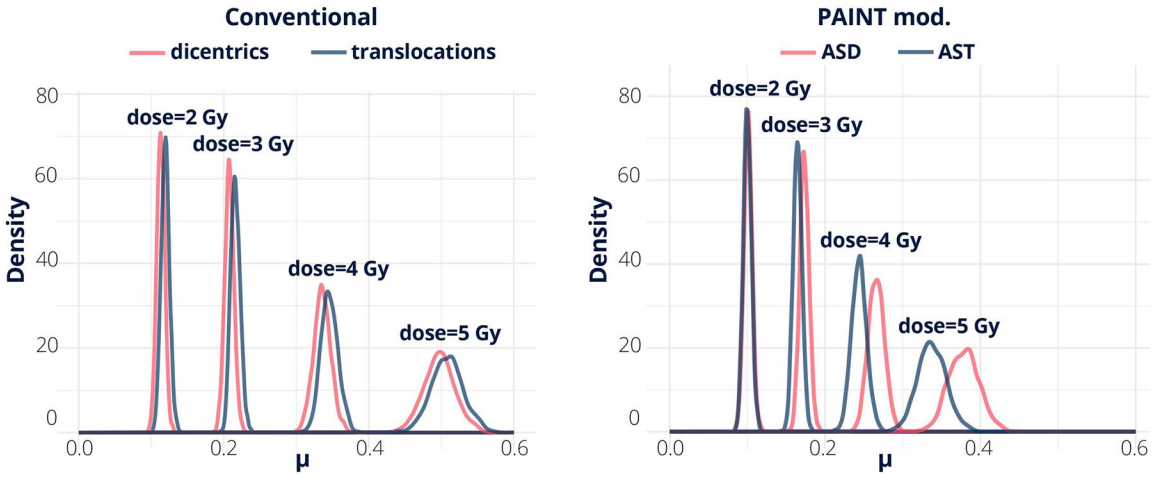

Figure 2. Posterior densities of the mean number of dicentrics, $\pi(\mu_{1d} \mid \mathbf{x}, \mathbf{y}, \boldsymbol{d}, \boldsymbol{p})$, and of the mean number of translocations, $\pi(\mu_{2d} \mid \mathbf{x}, \mathbf{y}, \boldsymbol{d}, \boldsymbol{p})$, given by the model for two scoring techniques.

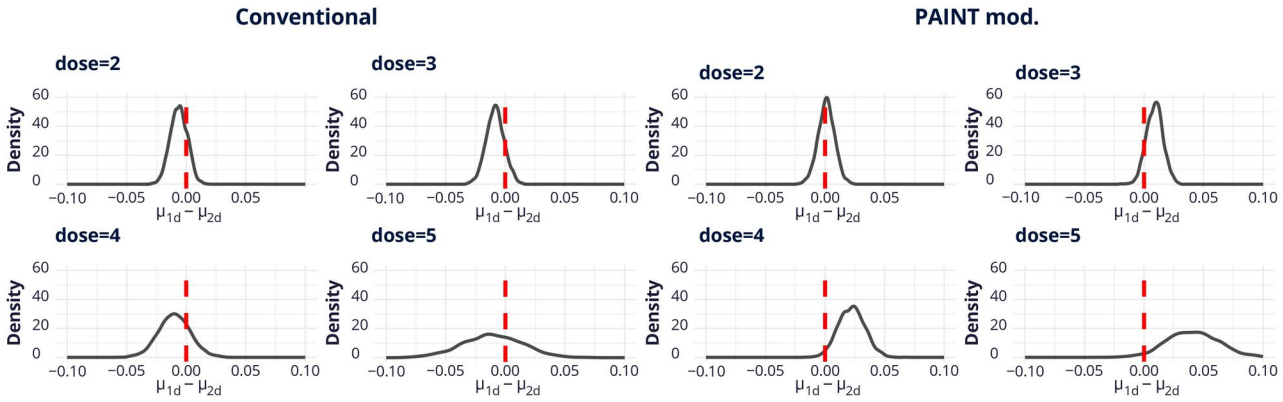

Figure 3. Posterior distribution of the difference between means of dicentrics and translocations $\pi(\mu_{1d} - \mu_{2d} \mid \mathbf{x}, \mathbf{y}, \boldsymbol{d}, \boldsymbol{p})$ given by the model for two scoring techniques. The red line is a reference line when $\mu_{1d} - \mu_{2d} = 0$.

Table 2. Posterior mean of the difference between means of dicentrics and translocations and 95% HDI for each dose and scoring technique.

	Conventional				PAINT mod.			
Dose (Gy)	2	3	4	5	2	3	4	5
Mean	−0.006	−0.008	−0.01	−0.011	0.001	0.009	0.022	0.041
HDI	[−0.019, 0.008]	[−0.022, 0.008]	[−0.035, 0.017]	[−0.06, 0.039]	[−0.013, 0.015]	[−0.004, 0.023]	[0.001, 0.044]	[−0.001, 0.085]

Table 3. Results of Bayes factor as defined by ratio (Equation (4)) for the conventional method of scoring and computed as the reciprocal of the fraction for the PAINT mod. method.

Dose (Gy)	2	3	4	5
Conventional	3.940	6.369	3.446	1.941
PAINT mod.	1.301	8.340	46.729	33.333

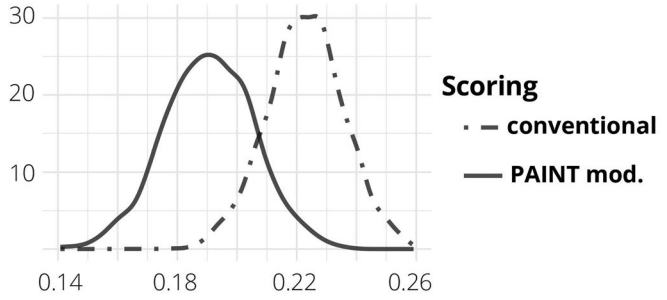

Figure 4. Posterior density of the survival index, γ, for the two methods of scoring.

Table 4. Actual proportion of irradiated cells ω estimated by the posterior mean of the survival γ given the dose of radiation d (in Gy) and the initial proportion p.

		Initial proportion of irradiated cells p					
Scoring method	Dose d (Gy)	1	0.875	0.75	0.5	0.25	0.125
conventional	2	1	0.818	0.658	0.39	0.176	0.084
	3	1	0.782	0.606	0.339	0.146	0.068
	4	1	0.742	0.552	0.291	0.120	0.055
	5	1	0.697	0.496	0.247	0.099	0.045
PAINT mod.	2	1	0.827	0.672	0.406	0.185	0.089
	3	1	0.798	0.629	0.361	0.158	0.075
	4	1	0.766	0.583	0.318	0.135	0.062
	5	1	0.730	0.536	0.278	0.114	0.052

results, for the PAINT mod. method, the Bayes factor was computed as the reciprocal of this fraction. According to the interpretation provided by Jeffreys (1961), the results offer substantial evidence supporting the hypothesis that μ_{1d} is lower than μ_{2d} for the conventional technique, a condition generally observed, as depicted in Figure 2. For the PAINT technique, when the mean of ASD exceeds the mean of AST, strong evidence is found indicating that μ_{1d} is greater than or equal to μ_{2d} for doses of 4 Gy and 5 Gy.

The current information about the survival index γ of the irradiated cells is represented by the posterior distribution in Figure 4. It is important to note that this survival rate, as defined in Section 2, is dose-dependent. Higher doses of radiation generally correspond to lower survival proportions, while lower doses tend to result in higher survival proportions. Additionally, the actual proportion of irradiated cells is also influenced by the initial proportion of irradiated cells as can be seen by Equation (3). Table 4 illustrates the relationship between the initial proportion of cells p, the received dose of radiation d, and the resulting actual proportion of surviving cells ω. These values are determined based on the mean value of the posterior density of the survival index γ. The estimated mean value of γ for the PAINT mod. method was 0.19, while for the conventional method it was 0.22. These results indicate a significant decrease in the proportion of irradiated cells that survived until metaphase. For example, when using the conventional method with a dose of 5 Gy and an initial proportion of 0.5, the estimated actual proportion of irradiated cells in the analyzed sample is approximately half of the initial proportion.

4. Discussion

As expected, the results of this study suggest that the choice of the scoring method significantly influences the analysis of the radiation-induced aberrations. However, the differences become less evident when the focus is on yields of aberrations using the same scoring technique. When using the conventional scoring method, the results suggest that there is a very small difference between the mean numbers of translocations and dicentrics observed. However, with the PAINT mod. method, a more pronounced variation in the results was found, but it is important to emphasize that our focus was solely on apparently simple aberrations. We believe that these results are primarily attributable to the fact that the conventional method does not differentiate between complex and simple chromosomal formations, whereas the PAINT mod. method does.

The prevailing understanding in past studies suggests that dicentrics and translocations have equal probability of appearing after chromosomal breaks induced by ionizing radiation (Lucas et al. 1996). However, it is important to note that there is no unanimous consensus of an equal formation ratio (1:1) and this theoretical assumption is occasionally questioned (Barquinero et al. 1998). Based on the findings from the PAINT mod. method, our results indicate that, when complex aberrations are excluded, there is a noteworthy difference in the mean number of dicentrics and translocations, particularly at higher radiation doses. Thus, the findings of this study directly impact biological dosimetry research, emphasizing the importance of selecting a specific biomarker for past dose assessment, as the interchangeability of results at high doses for dicentrics and translocations is not always guaranteed.

As the results suggest that the 1:1 ratio may not be valid, it may imply that translocations would occur more frequently than dicentrics in complex aberrations. It has been described that using FISH techniques the minimum detectable size is approximately 11 and 14 Mb for painted and unpainted material, respectively (Kodama et al. 1997). ASTs in which small fragments are exchanged may go unnoticed. On the contrary,

if two chromosomes break at their terminal part and form a dicentric chromosome, it will be clearly visible. This could explain the results for PAINT mod. method when the yield of AST is shifted left compared to ASD. However, the observation that this shift increases with dose could indicate that the different induction of AST and ASD could be related to the factors influencing the radiation-induced aberrations.

Several factors can impact the formation of different types of chromosomal aberrations. Some are specific to the radiation itself, including the pattern of energy deposition from various radiation types, as well as the dose and dose rate to which cells are exposed (Nikjoo et al. 1999; Anderson et al. 2000; Anderson et al. 2007; Stewart 2018; Liu 2022). Others are more related to how the deposited energy interacts with genomic material. Currently, it is widely accepted that chromosome aberrations result from the misrejoining of radiation-induced double-strand breaks (DSBs). Although after low-LET radiation, such as the X-rays used in the study by Duran et al. (2002), it can be assumed that energy deposition is randomly distributed into the nucleus, DSB production in the genome is not necessarily randomly distributed. After exposure to low-LET radiation, approximately 70% of DNA damage is attributed to radiation-induced free radicals. Because of their short diffusion distance and very short lifetimes, the impact of these free radicals is more commonly observed in regions of the genome where the chromatin is open (Chiu et al. 1986; Oleinick et al. 1994; Falk et al. 2008; Magnander et al. 2010; Saloua et al. 2014; Friedman et al. 2016).

In addition, the misrejoining of broken ends leading to chromosome exchanges is influenced by genome architecture and DSB processing. To form an inter-chromosome exchange-type aberration (such as dicentrics or translocations), broken ends should coexist in space and time. The use of FISH techniques has enabled the verification that, in interphase, each chromosome occupies a specific territory (Cremer and Cremer 2001). Inter-chromosome exchanges are more likely to occur in the boundaries of these territories, while intra-chromosome aberrations, such as ring chromosomes or inversions, are more prone to be produced within these territories (Sachs et al. 1993, 1997; Holley et al. 2002; Tello Cajiao et al. 2017).

Cells have four DNA-repair pathways to process DSBs (Iliakis et al. 2004, 2019), and it is hypothesized that the engagement of the different pathways depends on the chromatin destabilization generated by the DSBs. The aberrations considered in the present study come from G0 irradiated lymphocytes. Despite the stimulation of lymphocyte growth, it can be assumed that the primary repair pathway involved in the formation of these aberrations was the classical non-homologous end joining (c-NHEJ), and it is likely that a fraction of DNA ends is processed by the alternative end joining (alt-EJ). Both DNA-repair pathways join DNA ends independently of their origin, but while (c-NHEJ) is considered a fast repair mechanism, alt-EJ operates with slower kinetics. Consequently alt-EJ increases the probability of misrepairing and forming exchange type aberrations (Iliakis et al. 2019). When irradiating CHO cells with doses ranging from 0.5 to 6 Gy of X-rays, it was observed that complex aberrations appeared at higher doses (Darroudi et al. 1998). With the present results, we can hypothesize that at higher doses there will be greater destabilization of the genome, causing the alt-EJ repair mechanism to have a greater weight. This, in turn, is expected not only to result in more complex alterations but also in the formation of a higher number of simple dicentric type alterations (ASD) compared to simple translocations (AST). Consequently, further investigation and analysis are necessary to gain a better understanding of the underlying mechanisms and factors that influence the formation of dicentrics and translocations.

Author contributions

Conceptualization: D.M., P.P., and J.F.B.; methodology: D.M., P.P., C.A., and V.G.R.; software: D.M.; formal analysis: D.M.; resources: J.F.B.; data curation: J.F.B.; writing – original draft: D.M. and J.F.B.; writing – review and editing: D.M., P.P., C.A., V.G.R., and J.F.B.

Disclosure statement

No potential conflict of interest was reported by the author(s).

Funding

This work has been supported by grants: SBPLY/17/180501/000491 and SBPLY/21/180501/000241, funded by Consejería de Educación, Cultura y Deportes (JCCM, Spain) and Fondo Europeo de Desarrollo Regional; PID2019-106341GB-I00 and PID2022-136455NB-I00, funded by Ministerio de Ciencia e Innovación (Spain); CIAICO/2022/165, funded by Dirección General de Ciencia e Investigación (Generalitat Valenciana); BOE-A-2019-311 and SUBV-4/2023, funded by Consejo de Seguridad Nuclear. This work was also supported by the Agencia Estatal de Investigación [the Severo Ochoa and María de Maeztu Program for Centers and units of Excellence in R&D (CEX2020-001084-M)].

Notes on contributors

Dorota Młynarczyk, PhD student, Mathematician, PhD student at the Department of Mathematics, Faculty of Sciences, Universitat Autònoma de Barcelona, Bellaterra (Catalonia), Spain.

Pedro Puig, PhD, Mathematician, Professor at the Department of Mathematics and member of the Center de Recerca Matemàtica, Faculty of Sciences, Universitat Autònoma de Barcelona, Bellaterra (Catalonia), Spain.

Joan F. Barquinero, PhD, Biologist, Professor at the Department of Animal Biology, Plant Biology and Ecology, Faculty of Biosciences, Universitat Autònoma de Barcelona, Bellaterra (Catalonia), Spain.

Carmen Armero, PhD, Mathematician, Professor at the Department of Statistics and Operations Research, Faculty of Mathematics, Universitat de València, Burjassot (Valencian Community), Spain.

Virgilio Gómez-Rubio, PhD, Mathematician, Professor at the Department of Mathematics, School of Industrial Engineering, Universidad de Castilla-La Mancha, Albacete (Castilla-La Mancha), Spain.

ORCID

Dorota Młynarczyk http://orcid.org/0000-0002-7957-2567
Pedro Puig http://orcid.org/0000-0002-6607-9642

Joan F. Barquinero http://orcid.org/0000-0003-0084-5268
Carmen Armero http://orcid.org/0000-0001-9839-6442
Virgilio Gómez-Rubio http://orcid.org/0000-0002-4791-3072

Data availability statement

All data and computer code used for analysis during this study are included in Supplementary Material.

References

Anderson RM, Marsden SJ, Wright EG, Kadhim MA, Goodhead DT, Griffin CS. 2000. Complex chromosome aberrations in peripheral blood lymphocytes as a potential biomarker of exposure to high-LET alpha-particles. Int J Radiat Biol. 76(1):31–42. doi:10.1080/095530000138989

Anderson RM, Stevens DL, Sumption ND, Townsend KM, Goodhead DT, Hill MA. 2007. Effect of linear energy transfer (LET) on the complexity of alpha-particle-induced chromosome aberrations in human CD34+ cells. Radiat Res. 167(5):541–550. doi:10.1667/RR0813.1

Barquinero JF, Abe Y, Aneva N, Endesfelder D, Georgieva D, Goh V, Gregoire E, Hristova R, Lee Y, Martínez JS, et al. 2023. RENEB inter-laboratory comparison 2021: the FISH-based translocation assay. Radiat Res. 199(6):583–590. doi:10.1667/RADE-22-00203.1

Barquinero JF, Cigarrán S, Caballín MR, Braselmann H, Ribas M, Egozcue J, Barrios L. 1999. Comparison of X-ray dose–response curves obtained by chromosome painting using conventional and PAINT nomenclatures. Int J Radiat Biol. 75(12):1557–1566. doi:10.1080/095530099139160

Barquinero JF, Knehr S, Braselmann H, Figel M, Bauchinger M. 1998. DNA-proportional distribution of radiation-induced chromosome aberrations analysed by fluorescence in situ hybridization painting of all chromosomes of a human female karyotype. Int J Radiat Biol. 74(3):315–323. doi:10.1080/095530098141456

Bauchinger M, Schmid E, Zitzelsberger H, Braselmann H, Nahrstedt U. 1993. Radiation-induced chromosome aberrations analysed by two-colour fluorescence in situ hybridization with composite whole chromosome-specific DNA probes and a pancentromeric DNA probe. Int J Radiat Biol. 64(2):179–184. doi:10.1080/09553009314551271

Chiu SM, Friedman LR, Xue LY, Oleinick NL. 1986. Modification of DNA damage in transcriptionally active vs. bulk chromatin. Int J Radiat Oncol Biol Phys. 12(8):1529–1532. doi:10.1016/0360-3016(86)90209-9

Cornforth MN. 2001. Analyzing radiation-induced complex chromosome rearrangements by combinatorial painting. Radiat Res. 155(5):643–659. doi:10.1667/0033-7587(2001)155[0643:ARICCR]2.0.CO;2

Cremer T, Cremer C. 2001. Chromosome territories, nuclear architecture and gene regulation in mammalian cells. Nat Rev Genet. 2(4):292–301. doi:10.1038/35066075

Cremer T, Popp S, Emmerich P, Lichter P, Cremer C. 1990. Rapid metaphase and interphase detection of radiation-induced chromosome aberrations in human lymphocytes by chromosomal suppression in situ hybridization. Cytometry. 11(1):110–118. doi:10.1002/cyto.990110113

Darroudi F, Fomina J, Meijers M, Natarajan AT. 1998. Kinetics of the formation of chromosome aberrations in X-irradiated human lymphocytes, using PCC and FISH. Mutat Res. 404(1–2):55–65. doi:10.1016/s0027-5107(98)00095-5

Duran A, Barquinero JF, Caballín MR, Ribas M, Puig P, Egozcue J, Barrios L. 2002. Suitability of FISH painting techniques for the detection of partial-body irradiations for biological dosimetry. Radiat Res. 157(4):461–468. doi:10.1667/0033-7587(2002)157[0461:sofptf]2.0.co;2

Edwards AA, Lindholm C, Darroudi F, Stephan G, Romm H, Barquinero J, Barrios L, Caballin MR, Roy L, Whitehouse CA, et al. 2005. Review of translocations detected by FISH for retrospective biological dosimetry applications. Radiat Prot Dosimetry. 113(4):396–402. doi:10.1093/rpd/nch452

Falk M, Lukásová E, Kozubek S. 2008. Chromatin structure influences the sensitivity of DNA to gamma-radiation. Biochim Biophys Acta. 1783(12):2398–2414. doi:10.1016/j.bbamcr.2008.07.010

Fernández JL, Campos A, Goyanes V, Losada C, Veiras C, Edwards AA. 1995. X-ray biological dosimetry performed by selective painting of human chromosomes 1 and 2. Int J Radiat Biol. 67(3):295–302. doi:10.1080/09553009514550351

Friedman DA, Tait L, Vaughan AT. 2016. Influence of nuclear structure on the formation of radiation-induced lethal lesions. Int J Radiat Biol. 92(5):229–240. doi:10.3109/09553002.2016.1144941

Hall EJ, Giaccia AJ. 2006. Radiobiology for the radiologist. 6th ed. Philadelphia (PA): Lippincott Williams and Wilkins.

Holley WR, Mian IS, Park SJ, Rydberg B, Chatterjee A. 2002. A model for interphase chromosomes and evaluation of radiation-induced aberrations. Radiat Res. 158(5):568–580. doi:10.1667/0033-7587(2002)158[0568:amfica]2.0.co;2

[IAEA] International Atomic Energy Agency. 2001. Cytogenetic analysis for radiation dose assessment. Austria: IAEA.

[IAEA] International Atomic Energy Agency. 2011. Cytogenetic dosimetry: applications in preparedness for and response to radiation emergencies. Austria: IAEA.

Iliakis G, Mladenov E, Mladenova V. 2019. Necessities in the processing of DNA double strand breaks and their effects on genomic instability and cancer. Cancers. 11(11):1671. doi:10.3390/cancers11111671

Iliakis G, Wang H, Perrault AR, Boecker W, Rosidi B, Windhofer F, Wu W, Guan J, Terzoudi G, Pantelias G. 2004. Mechanisms of DNA double strand break repair and chromosome aberration formation. Cytogenet Genome Res. 104(1–4):14–20. doi:10.1159/000077461

[ISCN] An International System for Human Cytogenetic Nomenclature. 1985. Report of the Standing Committee on Human Cytogenetic Nomenclature. Birth Defects Orig Artic Ser. 21(1):1–117.

Jeffreys H. 1961. Theory of probability. 3rd ed. Oxford (UK): Clarendon Press.

Karlis D, Ntzoufras I. 2003. Analysis of sports data by using bivariate Poisson models. J R Stat Soc D. 52(3):381–393. doi:10.1111/1467-9884.00366

Kass RE, Raftery AE. 1995. Bayes factors. J Am Stat Assoc. 90(430):773–795. doi:10.1080/01621459.1995.10476572

Knehr S, Huber R, Braselmann H, Schraube H, Bauchinger M. 1999. Multicolour FISH painting for the analysis of chromosomal aberrations induced by 220 kV X-rays and fission neutrons. Int J Radiat Biol. 75(4):407–418. doi:10.1080/095530099140320

Knehr S, Zitzelsberger H, Bauchinger M. 1998. FISH-based analysis of radiation-induced chromosomal aberrations using different nomenclature systems. Int J Radiat Biol. 73(2):135–141. doi:10.1080/095530098142509

Kodama Y, Nakano M, Ohtaki K, Delongchamp R, Awa AA, Nakamura N. 1997. Estimation of minimal size of translocated chromosome segments detectable by fluorescence in situ hybridization. Int J Radiat Biol. 71(1):35–39. doi:10.1080/095530097144391

Kruschke J. 2014. Doing Bayesian data analysis: a tutorial with R, JAGS, and Stan. 2nd ed. Boston (MA): Academic Press/Elsevier.

Lee YH, Lee Y, Yoon HJ, Yang SS, Joo HM, Kim JY, Cho SJ, Jo WS, Jeong SK, Oh SJ, et al. 2021. An intercomparison exercise to compare scoring criteria and develop image databank for biodosimetry in South Korea. Int J Radiat Biol. 97(9):1199–1205. doi:10.1080/09553002.2021.1941384

Lindholm C, Luomahaara S, Koivistoinen A, Ilus T, Edwards AA, Salomaa S. 1998. Comparison of dose–response curves for chromosomal aberrations established by chromosome painting and conventional analysis. Int J Radiat Biol. 74(1):27–34. doi:10.1080/095530098141690

Liu G. 2022. Revision of cytogenetic dosimetry in the IAEA manual 2011 based on data about radio-sensitivity and dose-rate findings contributing. FASEB J. 36(11):e22621. doi:10.1096/fj.202200769RR

Lucas JN, Awa A, Straume T, Poggensee M, Kodama Y, Nakano M, Ohtaki K, Weier HU, Pinkel D, Gray J. 1992. Rapid translocation frequency analysis in humans decades after exposure to ionizing radiation. Int J Radiat Biol. 62(1):53–63. doi:10.1080/09553009214551821

Lucas JN, Chen AM, Sachs RK. 1996. Theoretical predictions on the equality of radiation-produced dicentrics and translocations detected by chromosome painting. Int J Radiat Biol. 69(2):145–153. doi:10.1080/095530096145977

Magnander K, Hultborn R, Claesson K, Elmroth K. 2010. Clustered DNA damage in irradiated human diploid fibroblasts: influence of chromatin organization. Radiat Res. 173(3):272–282. doi:10.1667/RR1891.1

Młynarczyk D, Puig P, Armero C, Gómez-Rubio V, Barquinero JF, Pujol-Canadell M. 2022. Radiation dose estimation with time-since-exposure uncertainty using the γ-H2AX biomarker. Sci Rep. 12(1):19877. doi:10.1038/s41598-022-24331-1

Moquet JE, Edwards AA, Lloyd DC, Hone P. 2000. The use of FISH chromosome painting for assessment of old doses of ionising radiation. Radiat Prot Dosimetry. 88(1):27–33. doi:10.1093/oxfordjournals.rpd.a033016

Nikjoo H, O'Neill P, Terrissol M, Goodhead DT. 1999. Quantitative modelling of DNA damage using Monte Carlo track structure method. Radiat Environ Biophys. 38(1):31–38. doi:10.1007/s004110050135

Oleinick NL, Balasubramaniam U, Xue L, Chiu S. 1994. Nuclear structure and the microdistribution of radiation damage in DNA. Int J Radiat Biol. 66(5):523–529. doi:10.1080/09553009414551561

Plummer M. 2003. JAGS: a program for analysis of Bayesian graphical models using Gibbs sampling. In: Hornik K, Leisch F, Zeileis A, editors. Proceedings of the 3rd International Workshop on Distributed Statistical Computing (DSC 2003); Mar 20–22; Technische Universität Wien, Vienna, Austria.

Pujol M, Barrios L, Puig P, Caballín MR, Barquinero JF. 2016. A new model for biological dose assessment in cases of heterogeneous exposures to ionizing radiation. Radiat Res. 185(2):151–162. doi:10.1667/RR14145.1

Sachs RK, Awa A, Kodama Y, Nakano M, Ohtaki K, Lucas JN. 1993. Ratios of radiation-produced chromosome aberrations as indicators of large-scale DNA geometry during interphase. Radiat Res. 133(3):345–350. doi:10.2307/3578220

Sachs RK, Brenner DJ, Chen AM, Hahnfeldt P, Hlatky LR. 1997. Intra-arm and interarm chromosome intrachanges: tools for probing the geometry and dynamics of chromatin. Radiat Res. 148(4):330–340. doi:10.2307/3579518

Saloua KS, Sonia G, Pierre C, Léon S, Darel HJ. 2014. The relative contributions of DNA strand breaks, base damage and clustered lesions to the loss of DNA functionality induced by ionizing radiation. Radiat Res. 181(1):99–110. doi:10.1667/RR13450.1

Savage JR, Papworth DG. 1982. Frequency and distribution studies of asymmetrical versus symmetrical chromosome aberrations. Mutat Res. 95(1):7–18. doi:10.1016/0027-5107(82)90062-8

Savage JR, Simpson P. 1994. On the scoring of FISH-"painted" chromosome-type exchange aberrations. Mutat Res. 307(1):345–353. doi:10.1016/0027-5107(94)90308-5

Schmid E, Zitzelsberger H, Braselmann H, Gray JW, Bauchinger M. 1992. Radiation-induced chromosome aberrations analysed by fluorescence in situ hybridization with a triple combination of composite whole chromosome-specific DNA probes. Int J Radiat Biol. 62(6):673–678. doi:10.1080/09553009214552621

Stewart RD. 2018. Induction of DNA damage by light ions relative to 60Co γ-rays. Int J Part Ther. 5(1):25–39. doi:10.14338/IJPT-18-00030

Tello Cajiao JJ, Carante MP, Bernal Rodriguez MA, Ballarini F. 2017. Proximity effects in chromosome aberration induction by low-LET ionizing radiation. DNA Repair. 58:38–46. doi:10.1016/j.dnarep.2017.08.007

Tucker JD, Morgan WF, Awa AA, Bauchinger M, Blakey D, Cornforth MN, Littlefield LG, Natarajan AT, Shasserre C. 1995. PAINT: a proposed nomenclature for structural aberrations detected by whole chromosome painting. Mutat Res. 347(1):21–24. doi:10.1016/0165-7992(95)90028-4